Adaptive Design of OFDM Radar Signal With Improved Wideband Ambiguity Function

Satyabrata Sen and Arye Nehorai, *Fellow, IEEE*

***Abstract*—We propose an adaptive technique to design the spectrum of an orthogonal frequency division multiplexing (OFDM) waveform to improve the radar's wideband ambiguity function (WAF). The adaptive OFDM signal yields a better auto-correlation function (ACF) that results into an improved delay (range) resolution for the radar system. First, we develop a mutlicarrier OFDM signal model and the corresponding WAF at the output of the matched filter, emphasizing that the received signal depends on the scattering parameters of the target. Then, we devise an optimization procedure to select the OFDM waveform such that the volume of the corresponding WAF best approximates the volume of a desired ambiguity function. We demonstrate the improvement in the resulting ambiguity function, along with the associated ACF, through numerical examples. We find that the optimization algorithm puts more signal energy at subcarriers in which the target response is weaker.**

***Index Terms*—Adaptive waveform design, multifrequency scattering, OFDM radar, wideband ambiguity function.**

I. Introduction

In this correspondence, we consider a mutlifrequency radar that employs an orthogonal frequency division multiplexing (OFDM) signal [1], and we compute its wideband ambiguity function (WAF) [2], [3] including the effects of the target response on the received signal. The motivation for employing multiple frequencies is that the different scattering centers of a target resonate differently at each frequency, and this also allows us to demonstrate the effects of target response on the WAF. Moreover, the use of a mutlicarrier OFDM signal improves the delay-resolution by a factor equal to the number of subcarriers [4], [5, Ch. 11]. In addition, we propose an algorithm to design the spectrum of the transmitting OFDM signal adaptively in order to improve its ambiguity profile.

A. Background

The advantage of multicarrier radar signaling has been well established in various applications, such as remote sensing of clouds and precipitation [6], detection of landmines [7], interpretation of an urban scene [8], etc. One of the ways to accomplish simultaneous use of several subcarriers is the OFDM signaling scheme, which employs multiple orthogonal signals in the time domain [9]. Although OFDM has been elaborately studied and commercialized in the digital communication field [10], it has not so widely been studied by the radar community apart from a few recent efforts [11]–[14].

The ambiguity function for radar was originally introduced by Ville [15]; however, it is generally referred to as Woodward's ambiguity function because of his popular work [16], [17]. According to Woodward, an ambiguity function is defined as a two-dimensional correlation between the transmitted narrowband signal and its time-delayed (related to target range) and frequency-shifted (related to target velocity) received version. Several literature interpret the ambiguity function as a matched filter response [18, Ch. 4], [19, Ch. 11], [20, Ch. 5], whereas a few others as a two-dimensional point-spread function [21], [22]. But in general, these formulations of the ambiguity function either do not include a scattering coefficient of the target in the received signal model, or they assume identical values for the scattering coefficients corresponding to different directions and/or frequencies. In our work, we follow a similar formulation of the ambiguity function but only after including the effect of different target responses at different frequencies.

Additionally, Woodward's version of the ambiguity function does not hold for large-bandwidth signals, such as OFDM signals. Target movements result in either expansion or compression in time for the wideband transmitted signal, and this effect can no longer be approximated by a simple "shift" in frequency. Therefore, in this work we follow the wideband ambiguity function (WAF) introduced by Kelley-Wishner [2] and Speiser [3]. Different properties of the WAF, similar to those of its narrowband counterpart, can be found in [23]–[26].

B. Outline

In Section II we describe the parametric models of the transmitted and received signals; then we compute their WAF. We emphasize that the received signal and hence the corresponding WAF at the output of the matched filter depend on the scattering parameters of the target. In Section III we propose an optimization algorithm to compute an adaptive OFDM waveform such that the volume of the corresponding WAF best approximates that of the desired ambiguity function. Our numerical examples, presented in Section IV, demonstrate the advantage of such an adaptive waveform design. Section V contains the conclusions and highlights of possible future work.

II. Signal Model and Wideband Ambiguity Function

In this section, we first introduce the transmitted and received signal models of an OFDM signaling system. Along with the delay and Doppler effects, the received signal model also incorporates the scattering coefficients of the target at multiple frequencies. Then, we compute the expressions of WAF for a single pulse and a coherent pulse train.

A. Signal Model

We consider a monostatic radar employing an OFDM signaling system [9] with L active subcarriers, a bandwidth of B Hz, and pulse duration of T seconds. Let $\boldsymbol{a} = [a_0, a_1, \ldots, a_{L-1}]^T$ contain the complex weights transmitted over different subcarriers, satisfying $\sum_{l=0}^{L-1} |a_l|^2 = 1$. Then the complex envelope of a single pulse can be represented as

$$\widetilde{s}(t) = \sum_{l=0}^{L-1} a_l \phi_l(t) \text{ where } \phi_l(t) = e^{j2\pi l \Delta f t} \tag{1}$$

and $\Delta f = B/L = 1/T$ denotes the subcarrier spacing. Let f_c be the carrier frequency of operation, the transmitted signal is given by

$$s(t) = 2\mathrm{Re}\left\{ \sum_{l=0}^{L-1} a_l e^{j2\pi f_l t} \right\} \tag{2}$$

where $f_l = f_c + l\Delta f$ represents the lth subcarrier frequency.

Manuscript received May 05, 2009; accepted August 23, 2009. First published September 18, 2009; current version published January 13, 2010. The associate editor coordinating the review of this manuscript and approving it for publication was Dr. Sergiy A. Vorobyov. This work was supported by the Department of Defense under the Air Force Office of Scientific Research MURI Grant FA9550-05-1-0443, and ONR Grant N000140810849.

The authors are with the Department of Electrical and Systems Engineering, Washington University in St. Louis, St. Louis, MO 63130 USA (e-mail: ssen3@ese.wustl.edu; nehorai@ese.wustl.edu).

Color versions of one or more of the figures in this correspondence are available online at http://ieeexplore.ieee.org.

Digital Object Identifier 10.1109/TSP.2009.2032456

Considering a far-field point target at distance r and relative velocity $\vec{v}$ with respect to the radar, the received signal in a noise-free scenario can be written as

$$y_1(t) = \sqrt{\gamma}\, s\left(\gamma(t-\tau)\right) \tag{3}$$

where $\gamma = 1+\beta$ accounts for the stretching or compressing in time of the reflected signal, $\beta = (2/c)\langle \widehat{\boldsymbol{u}}, \vec{v}\rangle$ represents the Doppler spreading factor, $\widehat{\boldsymbol{u}}$ is the unit direction-of-arrival (DOA) vector, $\tau = 2r/c$ is the roundtrip delay between the radar and the target, and c is the speed of propagation. Here $\langle ., . \rangle$ denotes the inner-product operator over the real vector space. Substituting (2) into (3), we get

$$\begin{aligned} y_1(t) &= 2\sqrt{\gamma}\mathrm{Re}\left\{\sum_{l=0}^{L-1} a_l e^{j2\pi f_l \gamma(t-\tau)}\right\} \\ &= 2\sqrt{\gamma}\mathrm{Re}\left\{\sum_{l=0}^{L-1} a_l e^{j2\pi l\Delta f \gamma(t-\tau)} e^{-j2\pi f_c\gamma\tau} e^{j2\pi f_c\gamma t}\right\} \\ &= 2\sqrt{\gamma}\mathrm{Re}\left\{\sum_{l=0}^{L-1} a_l \phi_l\left(\gamma(t-\tau)\right) e^{-j2\pi f_c\gamma\tau} e^{j2\pi\nu t} e^{j2\pi f_c t}\right\} \end{aligned}$$

where $\nu = f_c\beta$ represents the Doppler frequency. Hence, after demodulation the complex envelope of the received signal is

$$\widetilde{y}_1(t) = \sqrt{\gamma}\sum_{l=0}^{L-1} a_l \phi_l\left(\gamma(t-\tau)\right) e^{-j2\pi f_c\gamma\tau} e^{j2\pi\nu t}. \tag{4}$$

However, note that neither (3) nor (4) includes any parameter related to the target scattering coefficient. Therefore, denoting $\boldsymbol{x} = [x_0, x_1, \ldots, x_{L-1}]^T$ as a complex vector containing the scattering coefficients of the target at different subcarriers, we modify the expressions of the received signal as

$$y_2(t) = 2\sqrt{\gamma}Re\left\{\sum_{l=0}^{L-1} x_l a_l e^{j2\pi f_l\gamma(t-\tau)}\right\} \tag{5}$$

and the complex envelope as

$$\widetilde{y}_2(t) = \sqrt{\gamma}\sum_{l=0}^{L-1} x_l a_l \phi_l\left(\gamma(t-\tau)\right) e^{-j2\pi f_c\gamma\tau} e^{j2\pi\nu t}. \tag{6}$$

B. WAF of a Single Pulse

According to Kelley–Wishner [2], the wideband ambiguity function is defined as

$$\chi(\tau,\nu) \triangleq \sqrt{\gamma}\int_{-\infty}^{\infty} s_{anl}(t) s_{\mathrm{anl}}^*\left(\gamma(t-\tau)\right) dt \tag{7}$$

where $s_{\mathrm{anl}}(t)$ represents the analytic signal corresponding to $s(t)$ and '$*$' is the complex conjugate operator. On the assumption that the complex envelope $\widetilde{s}(t)$ is perfectly bandlimited in comparison with the carrier frequency f_c, which is true for most radar signals [27], we can consider $s_{anl}(t) = \widetilde{s}(t)e^{j2\pi f_c t}$. Therefore, (7) can be simplified to

$$\chi(\tau,\nu) = e^{j2\pi f_c\gamma\tau}\left[\sqrt{\gamma}\int_{-\infty}^{\infty} \widetilde{s}(t)\widetilde{s}^*\left(\gamma(t-\tau)\right) e^{-j2\pi\nu t} dt\right]. \tag{8}$$

Sometimes this expression is referred to as the output of an optimum detector filter matched to zero delay and zero Doppler [22], with only the term within the square bracket in (8) labeled as the WAF [28]. Alternatively, in some other literatures the WAF is defined as the magnitude or magnitude-squared of the term within the square bracket in (8) [29].

Now, incorporating the effects of the target response in the received signal, we redefine the WAF at the output of the matched filter as follows:

$$\begin{aligned} &\chi_{\mathrm{MF}}(\tau,\nu,\boldsymbol{a},\boldsymbol{x}) \\ &\quad = e^{j2\pi f_c\gamma\tau}\left[\sqrt{\gamma}\int_{T\min}^{T\max}\left(\sum_{l_1=0}^{L-1} a_{l_1}\phi_{l_1}(t)\right)\right. \\ &\qquad\qquad \left.\cdot\left(\sum_{l_2=0}^{L-1} x_{l_2}^* a_{l_2}^* \phi_{l_2}^*\left(\gamma(t-\tau)\right)\right) e^{-j2\pi\nu t} dt\right], \\ &\quad = \sum_{l_1=0}^{L-1}\sum_{l_2=0}^{L-1} a_{l_1} a_{l_2}^* x_{l_2}^* \chi_{\phi_{l_1}\phi_{l_2}}(\tau,\nu) \end{aligned} \tag{9}$$

where $T_{\min} = \max(0,\tau)$, $T_{\max} = \min(T, T/\gamma+\tau)$, and

$$\begin{aligned} \chi_{\phi_{l_1}\phi_{l_2}}(\tau,\nu) &= e^{j2\pi f_c\gamma\tau} \\ &\quad\cdot\left[\sqrt{\gamma}\int_{T_{\min}}^{T\max} \phi_{l_1}(t)\phi_{l_2}^*(\gamma(t-\tau)) e^{-j2\pi\nu t} dt\right] \end{aligned}$$

denotes the cross-ambiguity function between $\phi_{l_1}(t)$ and $\phi_{l_2}(t)$, having a similar form as (8). Note that in (9) we explicitly parametrize $\chi_{\mathrm{MF}}(\cdot)$ in terms of $\boldsymbol{x}$ to emphasize that it depends on the scattering coefficients of the target. In addition, $\chi_{\mathrm{MF}}(\cdot)$ also depends on $\boldsymbol{a}$. This parametrization is realistic and also enables us to adaptively design the spectrum of the transmitted OFDM signal to improve the corresponding ambiguity profile, which will be discussed in Section III. We can further simplify (9) to the following (see Appendix A):

$$\chi_{\mathrm{MF}}(\tau,\nu,\boldsymbol{a},\boldsymbol{x}) = \chi_{\mathrm{MF}}^{(\mathrm{ml})}(\tau,\nu,\boldsymbol{a},\boldsymbol{x}) + \chi_{\mathrm{MF}}^{(\mathrm{sl})}(\tau,\nu,\boldsymbol{a},\boldsymbol{x}) \tag{10}$$

where

$$\begin{aligned} &\chi_{\mathrm{MF}}^{(\mathrm{ml})}(\tau,\nu,\boldsymbol{a},\boldsymbol{x}) \\ &\quad\triangleq \sqrt{\gamma}T_{\mathrm{diff}}\sum_{l=0}^{L-1} x_l^*|a_l|^2 \mathrm{sinc}\left[f_l\beta T_{\mathrm{diff}}\right] e^{j2\pi\left[f_l\gamma\tau-\beta f_l T_{\mathrm{avg}}\right]} \\ &\chi_{\mathrm{MF}}^{(\mathrm{sl})}(\tau,\nu,\boldsymbol{a},\boldsymbol{x}) \\ &\quad\triangleq \sqrt{\gamma}T_{\mathrm{diff}} \\ &\qquad\cdot\sum_{l_1=0}^{L-1}\sum_{\substack{l_2=0\\ l_2\neq l_1}}^{L-1} x_{l_2}^* a_{l_1} a_{l_2}^* \mathrm{sinc}\left[\{f_{l_2}\beta+(l_2-l_1)\Delta f\}T_{\mathrm{diff}}\right] \\ &\qquad\cdot e^{j2\pi\left[f_{l_2}\gamma\tau-\{\beta f_{l_2}+(l_2-l_1)\Delta f\}T_{\mathrm{avg}}\right]} \end{aligned}$$

and $T_{\mathrm{diff}} = T_{\max} - T_{\min}$, $T_{\mathrm{avg}} = (T_{\max}+T_{\min})/2$. If we plot separately we can see that $\chi_{\mathrm{MF}}^{(\mathrm{ml})}(\cdot)$ produces the mainlobe of the WAF while $\chi_{\mathrm{MF}}^{(\mathrm{sl})}(\cdot)$ produces the sidelobes.

Special Case: For a conventional radar employing a single carrier frequency f_c, (10) can be simplified to

$$\chi_{\mathrm{MF}}(\tau,\nu,\boldsymbol{a},\boldsymbol{x}) = \sqrt{\gamma}T_{\mathrm{diff}}x^*|a|^2\mathrm{sinc}\left[f_c\beta T_{\mathrm{diff}}\right] e^{j2\pi f_c\left(\gamma\tau-\beta T_{\mathrm{avg}}\right)}$$

and therefore, the expression of the normalized WAF,

$$\frac{\chi_{\mathrm{MF}}(\tau,\nu,\boldsymbol{a},\boldsymbol{x})}{\chi_{\mathrm{MF}}(0,0,\boldsymbol{a},\boldsymbol{x})} = \frac{T_{\mathrm{diff}}}{T_{\mathrm{diff}}^{(0)}}\,\mathrm{sinc}\left(\nu T_{\mathrm{diff}}\right) e^{-j2\pi\nu T_{\mathrm{avg}}}, \tag{11}$$

does not depend on the scattering coefficients of the target. Here $T_{\mathrm{diff}}^{(0)}$ is T_{diff} evaluated at $\tau = 0$.

C. WAF of a Pulse Train

The Doppler-resolution of the ambiguity function is improved when we transmit a coherent pulse train. The complex envelope of a train of N identical pulses can be described as

$$\widetilde{s}_N(t) = \sum_{n=0}^{N-1} \widetilde{s}(t - nT_{\mathrm{PRI}}) \tag{12}$$

where T_{PRI} is the pulse repetition interval (PRI). Then, the transmitted signal is given by

$$\begin{aligned} s_N(t) &= 2\mathrm{Re}\left\{\widetilde{s}_N(t)e^{j2\pi f_c t}\right\} \\ &= 2\mathrm{Re}\left\{\sum_{n=0}^{N-1} \widetilde{s}(t - nT_{\mathrm{PRI}})\, e^{j2\pi f_c t}\right\}. \end{aligned} \tag{13}$$

Using the expression of the analytic signal corresponding to $s_N(t)$ in (7), we can formulate the WAF of a coherent pulse train as follows:

$$\begin{aligned} &\chi_N(\tau,\nu) \\ &= \sqrt{\gamma}\int_{-\infty}^{\infty}\left[\sum_{n_1=0}^{N-1}\widetilde{s}(t - n_1T_{\mathrm{PRI}})\, e^{j2\pi f_c t}\right] \\ &\quad\cdot\left[\sum_{n_2=0}^{N-1}\widetilde{s}^{*}\left(\gamma(t-\tau) - n_2T_{\mathrm{PRI}}\right) e^{j2\pi f_c\gamma(t-\tau)}\right] dt \\ &= \sum_{n_1=0}^{N-1}\sum_{n_2=0}^{N-1}\chi\left(\tau + \left(\frac{n_2}{\gamma} - n_1\right)T_{\mathrm{PRI}},\nu\right) e^{-j2\pi(n_2-n_1)T_{\mathrm{PRI}}} \end{aligned} \tag{14}$$

where $\chi(\cdot)$ is the WAF of a single pulse as defined in (8). See Appendix B for the derivation of (14).

Following a similar type of derivation, including the effects of the target response in the received signal, we can modify the expression of WAF for a coherent pulse train as follows:

$$\begin{aligned} &\chi_{\mathrm{MF}_N}(\tau,\nu,\boldsymbol{a},\boldsymbol{x}) \\ &= \sum_{n_1=0}^{N-1}\sum_{n_2=0}^{N-1}\chi_{\mathrm{MF}}\left(\tau + \left(\frac{n_2}{\gamma} - n_1\right)T_{\mathrm{PRI}},\nu,\boldsymbol{a},\boldsymbol{x}\right) \\ &\quad\cdot e^{-j2\pi f_c(n_2-n_1)T_{\mathrm{PRI}}}, \\ &= \sum_{n_1=0}^{N-1}\sum_{n_2=0}^{N-1}\left[\sum_{l_1=0}^{L-1}\sum_{l_2=0}^{L-1} a_{l_1}a_{l_2}^{*}x_{l_2}^{*}\right. \\ &\qquad\left.\cdot\chi_{\phi_{l_1}\phi_{l_2}}\left(\tau + \left(\frac{n_2}{\gamma} - n_1\right)T_{\mathrm{PRI}},\nu\right)\right] \\ &\quad\cdot e^{-j2\pi f_c(n_2-n_1)T_{\mathrm{PRI}}}, \\ &= \sum_{l_1=0}^{L-1}\sum_{l_2=0}^{L-1} a_{l_1}a_{l_2}^{*}x_{l_2}^{*}\chi_{\phi_{l_1}\phi_{l_2}{}_N}(\tau,\nu) \end{aligned} \tag{15}$$

where

$$\begin{aligned} &\chi_{\phi_{l_1}\phi_{l_2}{}_N}(\tau,\nu) \\ &= \sum_{n_1=0}^{N-1}\sum_{n_2=0}^{N-1}\chi_{\phi_{l_1}\phi_{l_2}}\left(\tau + \left(\frac{n_2}{\gamma} - n_1\right)T_{\mathrm{PRI}},\nu\right) \\ &\quad\cdot e^{-j2\pi f_c(n_2-n_1)T_{\mathrm{PRI}}} \end{aligned} \tag{16}$$

denotes the cross-ambiguity function between two coherent pulse trains of $\phi_{l_1}(t)$ and $\phi_{l_2}(t)$. In the rest of the correspondence we will consider the magnitude squared of (15), $|\chi_{\mathrm{MF}_N}(\cdot)|^2$, as the expression of WAF.

III. Adaptive Waveform Design

In this section, we describe an optimization approach to adaptively design the spectrum of an OFDM signal such that the volume of the corresponding WAF best approximates the volume of a desired ambiguity profile.

The problem of synthesizing a waveform to satisfy a desired ambiguity function has been addressed extensively over the years [14], [30]–[37]. Wilcox [30] and Sussman [31] approached this problem to approximate the desired ambiguity profile in the least-squared (LS) sense. Their optimization procedure stretches over the entire (τ,ν) plane, and hence the resultant waveform can produce an "all-purpose" ambiguity function that would be more or less suitable for any radar applications [31]. However, in many situations, it is not necessary to have a certain ambiguity shape for all values of τ and ν. Recently, Gladkova *et al.* [36], [37] extended Wilcox's LS approach, restricting the optimization procedure over some limited subregions in the (τ,ν) plane, particularly surrounding the mainlobe.

In this work, we seek to find an OFDM waveform satisfying $\sum_{l=0}^{L-1}|a_l|^2 = 1$, such that the error between the volumes of the resulting WAF and desired ambiguity function is the minimum. Instead of covering the entire (τ,ν) plane, we also limit the volume computations over a subregion, $\mathcal{R}$, containing the origin. Denoting the desired ambiguity function as $\chi_{\mathrm{opt}}(\tau,\nu)$, we can state the optimization problem as follows:

$$\begin{aligned} &\boldsymbol{a}_{\mathrm{opt}}(\boldsymbol{x}) \\ &\quad= \underset{\boldsymbol{a}}{\mathrm{argmin}}\int_{\mathcal{R}}\left|\,|\chi_{\mathrm{opt}}(\tau,\nu)|^2 - |\chi_{MF_N}(\tau,\nu,\boldsymbol{a},\boldsymbol{x})|^2\right| d\tau d\nu, \\ &\quad\text{subject to}\ \sum_{l=0}^{L-1}|a_l|^2 = 1 \text{ and } |a_l|^2 > \epsilon \quad \forall\, l \end{aligned} \tag{17}$$

where ϵ is a small positive quantity (close to zero) ensuring transmission over all L frequency channels. We use numerical methods to solve for the optimized variables, $\boldsymbol{a}_{\mathrm{opt}}$, that depend on the scattering coefficients of the target and hence comply with the philosophy of "adaptive" design.

In some particular cases, when $|\chi_{\mathrm{opt}}(\cdot)|^2 < |\chi_{\mathrm{MF}_N}(\cdot)|^2$ holds true over the entire subregion $\mathcal{R}$ (e.g., $\chi_{\mathrm{opt}}(\tau,\nu) = \delta(\tau,\nu)$), we can further simplify (17) to the following:

$$\begin{aligned} &\boldsymbol{a}_{\mathrm{opt}}(\boldsymbol{x}) = \underset{\boldsymbol{a}}{\mathrm{argmin}}\int_{\mathcal{R}}|\chi_{\mathrm{MF}_N}(\tau,\nu,\boldsymbol{a},\boldsymbol{x})|^2\, d\tau d\nu, \\ &\text{subject to}\ \sum_{l=0}^{L-1}|a_l|^2 = 1 \text{ and } |a_l|^2 > \epsilon \quad \forall\, l, \\ &\boldsymbol{a}_{\mathrm{opt}}(\boldsymbol{x}) = \underset{\boldsymbol{a}}{\mathrm{argmin}}\sum_{l_1=0}^{L-1}\sum_{l_2=0}^{L-1}\sum_{l_3=0}^{L-1}\sum_{l_4=0}^{L-1} a_{l_1}a_{l_2}^{*}a_{l_3}^{*}a_{l_4}x_{l_2}^{*}x_{l_4} \\ &\quad\cdot\int_{\mathcal{R}}\chi_{\phi_{l_1}\phi_{l_2}{}_N}(\tau,\nu)\chi_{\phi_{l_3}\phi_{l_4}{}_N}^{*}(\tau,\nu)d\tau d\nu. \end{aligned} \tag{18}$$

Hence, this leads to a minimization procedure having fourth order form, similar to that presented in [37], with the incorporation of the target scattering coefficients. However, from mathematical perspective our method can be categorized as an $\mathcal{L}_1$ minimization, while that of [37] as an $\mathcal{L}_2$ minimization.

The convergence time of (17) strongly depends on the area of subregion $\mathcal{R}$ and the shape of the desired ambiguity function $\chi_{\mathrm{opt}}(\tau,\nu)$. If the knowledge of the target response is known *a priori*, we can use an offline computation of (17) extending over a larger area of $\mathcal{R}$ and considering an impulse-shaped $\chi_{\mathrm{opt}}(\cdot)$. In real-time processing, when we need to compute $\boldsymbol{a}_{\mathrm{opt}}$ based on the estimated value of $\boldsymbol{x}$ from the

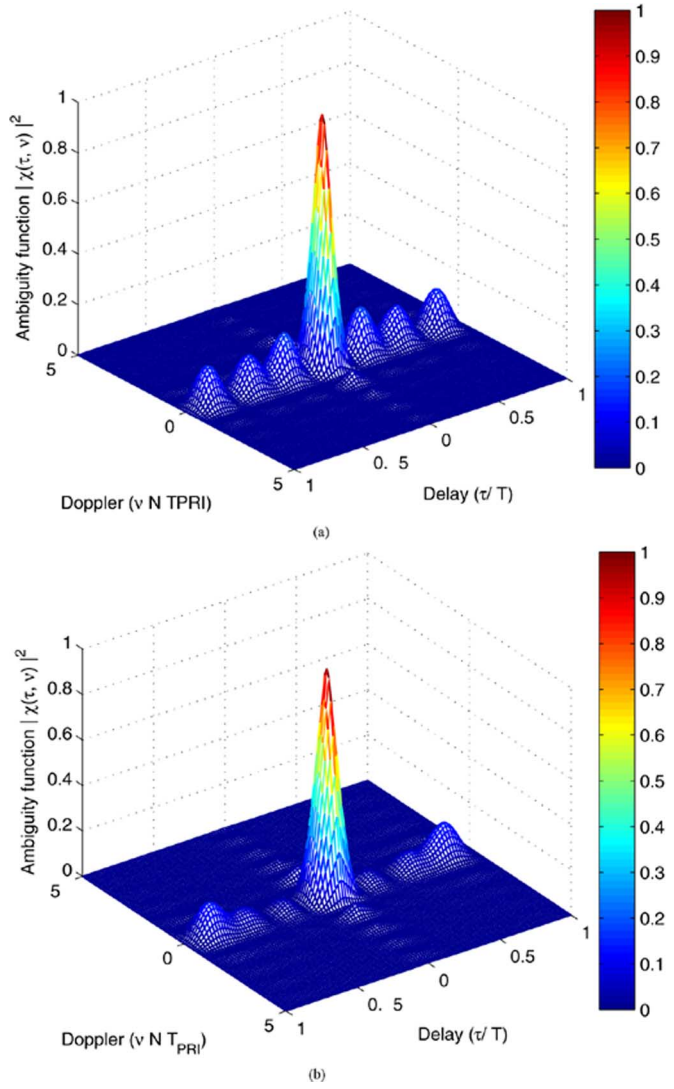

Fig. 1. Plots of wideband ambiguity functions for (a) fixed and (b) adaptive waveforms over a region $\mathcal{R} = \{|\tau| \leq T, |\nu| \leq 1/(2T_{\rm PRI})\}$.

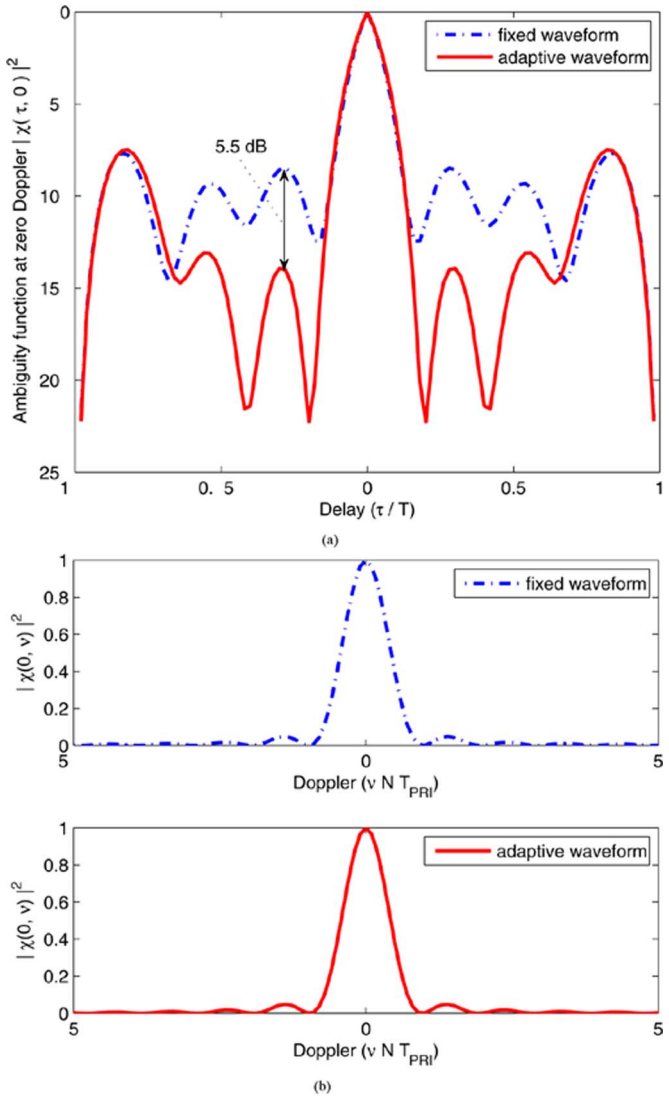

Fig. 2. (a) Zero-Doppler cuts (auto-correlation functions) and (b) zero-delay cuts of the wideband ambiguity functions corresponding to the adaptive and fixed waveforms.

previous radar dwell, it would be practical to restrict $\mathcal{R}$ to a smaller region (e.g., $|\tau| \leq T, |\nu| \leq 1/(2T_{\rm PRI})$) and not to choose an "idealistic" shape of $\chi_{\rm opt}(\cdot)$.

IV. Numerical Results

We present simulation results to demonstrate the advantage of adaptive waveform design, in the form of an improved ambiguity profile. We consider an OFDM radar operating with the following specifications: carrier frequency $f_c = 1$ GHz; available bandwidth $B = 125$ MHz; number of subcarriers $L = 4$; subcarrier spacing $\Delta f = B/(L+1) = 25$ MHz; pulsewidth $T = 1/\Delta f = 40$ ns; pulse repetition interval $T_{\rm PRI} = 20\ \mu$s; number of coherent pulses $N = 10$. To evaluate $\boldsymbol{a}_{\rm opt}$ we used $\mathcal{R} := \{|\tau| \leq T, |\nu| \leq 1/(2T_{\rm PRI})\}$ and an impulse-like $\chi_{\rm opt}(\tau, \nu)$ that has value 1 at the origin but zero everywhere else. We realized the entries of $\boldsymbol{x}$ from a $\mathcal{N}(0,1)$ distribution. The results presented in Figs. 1 and 2 were obtained using the numerical optimization solver of MATLAB and after averaging over 50 such independent realizations of $\boldsymbol{x}$. We compared this adaptively designed WAF with that obtained from a fixed waveform that employs $a_l = 1/\sqrt{L}\ \forall l$.

Fig. 1(b) depicts the WAF obtained from the optimized waveform following (17). This ambiguity function shows a considerable improvement in comparison with the one shown in Fig. 1(a), which was obtained from a fixed waveform. Numerically, the normalized volume under the ambiguity profile reduces from unity to 0.806. The zero-delay and zero-Doppler cut plots of these ambiguity profiles are shown in Fig. 2. From Fig. 2(a) it is quite evident that the adaptive waveform results in a much better auto-correlation function. The first sidelobe level of the ambiguity function corresponding to the adaptive waveform is 5.5 dB down with respect to those of its counterpart for fixed waveform. The zero-delay cut plots in Fig. 2(b) suggest that there is no change in the Doppler resolution, as we expect, due to adaptive waveform design.

For further insight into the optimization procedure, we looked into the energy distributions of the adaptive waveform and target response over different subcarriers. For example, in a particular sample run we had $|x_l| = \{6.42, 1.03, 4.23, 5.66\}$, and the optimization algorithm (17) resulted in $|a_l| = \{0.24, 0.80, 0.42, 0.29\}$ when initialized with $a_l = 1/\sqrt{L} = 0.50\ \forall\ l$. From this we can make two observations: i) the sample variance of $|a_l x_l|$ reduces from 1.06 to 0.13 and ii) the

redistribution energy occurs with more signal energy to that particular subcarrier in which the target response is weaker and less signal energy to the subcarrier over which the target response is already stronger.

V. Conclusion

We proposed an optimization algorithm to compute an adaptive radar waveform such that the volume of the corresponding wideband ambiguity function best approximates the volume of a desired ambiguity function over a region in the delay-Doppler plane. For this purpose, we considered an OFDM radar and developed the received signal model while incorporating the scattering coefficients of the target at multiple frequencies. We emphasize that the expression of the wideband ambiguity function at the output of a matched filter must include the target response along with delay and Doppler. We numerically demonstrated the advantage of adaptive waveform design. We concluded that the optimization algorithm puts more signal energy at that particular subcarrier in which the target response is weaker, thus increasing the possibility of a better target return. In future work, we will include several other characteristics of the wideband ambiguity function, such as mainlobe width and sidelobe level, in the waveform designing criterion.

Appendix A

The term within the square bracket in (9) can be written as

$$\begin{aligned}
&\sqrt{\gamma}\int_{-\infty}^{\infty}\left(\sum_{l_1=0}^{L-1}a_{l_1}e^{j2\pi l_1\Delta f t}\right)\left(\sum_{l_2=0}^{L-1}x_{l_2}^{*}a_{l_2}^{*}e^{-j2\pi l_2\Delta f\gamma(t-\tau)}\right)\\
&\quad\cdot e^{-j2\pi\nu t}dt\\
&\quad=\sqrt{\gamma}\sum_{l=0}^{L-1}x_l^{*}\left|a_l\right|^2e^{j2\pi l\Delta f\gamma\tau}\int_{T_{\min}}^{T_{\max}}e^{-j2\pi(l\Delta f+f_c)\beta t}dt\\
&\qquad+\sqrt{\gamma}\sum_{l_1=0}^{L-1}\sum_{\substack{l_2=0\\ l_2\neq l_1}}^{L-1}x_l^{*}a_{l_1}a_{l_2}^{*}e^{j2\pi l_2\Delta f\gamma\tau}\\
&\qquad\cdot\int_{T_{\min}}^{T_{\max}}e^{-j2\pi[(l_2\Delta f+f_c)\beta+(l_2-l_1)\Delta f]t}dt. \qquad \text{(A1)}
\end{aligned}$$

Using the definitions of $f_l, T_{\min}, T_{\max}, T_{\text{diff}}, T_{\text{avg}}$, and the following integration result:

$$\int_{T_{\min}}^{T_{\max}}e^{-j2\pi ft}dt=T_{\text{diff}}\operatorname{sinc}\left(fT_{\text{diff}}\right)e^{-j2\pi fT_{\text{avg}}}, \qquad \text{(A2)}$$

we get the expressions of $\chi_{\text{MF}}^{(\text{ml})}(\tau,\nu,\boldsymbol{a},\boldsymbol{x})$ and $\chi_{\text{MF}}^{(\text{sl})}(\tau,\nu,\boldsymbol{a},\boldsymbol{x})$.

Appendix B

The derivation of (14) involves the following steps:

$$\begin{aligned}
\chi_N(\tau,\nu)&=\sqrt{\gamma}\int_{-\infty}^{\infty}\left[\sum_{n_1=0}^{N-1}\widetilde{s}\left(t-n_1T_{\text{PRI}}\right)e^{j2\pi f_ct}\right]\\
&\qquad\cdot\left[\sum_{n_2=0}^{N-1}\widetilde{s}^{*}\left(\gamma(t-\tau)-n_2T_{\text{PRI}}\right)e^{j2\pi f_c\gamma(t-\tau)}\right]dt\\
&=\sqrt{\gamma}e^{j2\pi f_c\gamma\tau}\sum_{n_1=0}^{N-1}\sum_{n_2=0}^{N-1}\int_{-\infty}^{\infty}\widetilde{s}(t-n_1T_{\text{PRI}})\\
&\qquad\cdot\widetilde{s}^{*}\left(\gamma(t-\tau)-n_2T_{\text{PRI}}\right)e^{j2\pi\nu t}dt.
\end{aligned}$$

Using a change of variable with $p=t-n_1T_{\text{PRI}}$ we get

$$\begin{aligned}
&\chi_N(\tau,\nu)\\
&\quad=\sqrt{\gamma}e^{j2\pi f_c\gamma\tau}\sum_{n_1=0}^{N-1}\sum_{n_2=0}^{N-1}e^{j2\pi\nu n_1T_{\text{PRI}}}\int_{-\infty}^{\infty}\widetilde{s}(p)\\
&\qquad\cdot\widetilde{s}^{*}\left(\gamma(p+n_1T_{\text{PRI}}-\tau)-n_2T_{\text{PRI}}\right)e^{j2\pi\nu p}dp\\
&\quad=\sum_{n_1=0}^{N-1}\sum_{n_2=0}^{N-1}e^{j2\pi\nu n_1T_{\text{PRI}}}e^{j2\pi f_c\gamma(n_2/\gamma-n_1)T_{\text{PRI}}}\\
&\qquad\cdot\left[\sqrt{\gamma}e^{j2\pi f_c\gamma(\tau+(n_2/\gamma-n_1)T_{\text{PRI}})}\int_{-\infty}^{\infty}\widetilde{s}(p)\right.\\
&\qquad\left.\cdot\widetilde{s}^{*}\left(\gamma\left(p-\left[\tau+\left(\frac{n_2}{\gamma+n_1}\right)T_{\text{PRI}}\right]\right)\right)e^{j2\pi\nu p}dp\right]. \qquad \text{(B1)}
\end{aligned}$$

The term in the square bracket has a similar form as (8) when τ is replaced with $(\tau+(n_2/\gamma-n_1)T_{\text{PRI}})$, and $\nu n_1T_{\text{PRI}}+f_c\gamma(n_2/\gamma-n_1)T_{\text{PRI}}=f_c\left(n_2-n_1\right)T_{\text{PRI}}$. Hence, (B1) reduces to (14).

References

[1] A. Pandharipande, "Principles of OFDM," *IEEE Potentials*, vol. 21, no. 2, pp. 16–19, Apr. 2002.

[2] E. J. Kelly and R. P. Wishner, "Matched-filter theory for high-velocity accelerating targets," *IEEE Trans. Mil. Electron.*, vol. 9, pp. 56–69, Jan. 1965.

[3] J. Speiser, "Wide-band ambiguity functions (Corresp.)," *IEEE Trans. Inf. Theory*, vol. 13, no. 1, pp. 122–123, Jan. 1967.

[4] N. Levanon, "Multifrequency complementary phase-coded radar signal," *Proc. Inst. Electr. Eng.—Radar, Sonar, Navig.*, vol. 147, no. 6, pp. 276–284, Dec. 2000.

[5] N. Levanon and E. Mozeson, *Radar Signals*. Hoboken, NJ: Wiley-IEEE Press, 2004.

[6] N. Majurec, S. M. Sekelsky, S. J. Frasier, and S. A. Rutledge, "The advanced multi-frequency radar (AMFR) for remote sensing of clouds and precipitation," presented at the 32nd Conf. Radar Meteorology, Albuquerque, NM, 2004, Paper P1R.6.

[7] P. V. Genderen, P. Hakkaart, J. V. Heijenoort, and G. P. Hermans, "A multi frequency radar for detecting landmines: Design aspects and electrical performance," in *Proc. 31st Eur. Microwave Conf.*, 2001, vol. 2, pp. 249–252.

[8] M. L. Bryan, "Interpretation of an urban scene using multi-channel radar imagery," *Remote Sens. Environ.*, vol. 4, no. 1, pp. 49–66, 1975.

[9] S. B. Weinstein and P. M. Ebert, "Data transmission by frequency-division multiplexing using the discrete Fourier transform," *IEEE Trans. Commun. Technol.*, vol. 19, pp. 476–488, Oct. 1971.

[10] B. L. Floch, R. Halbert-Lassalle, and D. Castelain, "Digital sound broadcasting to mobile receivers," *IEEE Trans. Consum. Electron.*, vol. 35, no. 3, pp. 493–503, Aug. 1989.

[11] G. E. A. Franken, H. Nikookar, and P. V. Genderen, "Doppler tolerance of OFDM-coded radar signals," in *Proc. 3rd Eur. Radar Conf.*, Manchester, U.K., Sep. 13–15, 2006, pp. 108–111.

[12] D. S. Garmatyuk, "Simulated imaging performance of UWB SAR based on OFDM," in *Proc. IEEE 2006 Int. Conf. Ultra-Wideband*, Sep. 2006, pp. 237–242.

[13] J. P. Stralka, "Applications of orthogonal frequency-division multiplexing (OFDM) to radar," Ph.D. dissertation, The Johns Hopkins University, Baltimore, MD, 2008.

[14] M. Sebt, A. Sheikhi, and M. Nayebi, "Orthogonal frequency-division multiplexing radar signal design with optimised ambiguity function and low peak-to-average power ratio," *IET Radar, Sonar, Navig.*, vol. 3, no. 2, pp. 122–132, Apr. 2009.

[15] J. Ville, "Théorie et application de la notion de signal analytique," *Cables et Transmission*, vol. 2, no. 1, pp. 61–74, 1948.

[16] P. M. Woodward, *Probability and Information Theory, With Applications to Radar*. New York: McGraw-Hill, 1953.

[17] P. M. Woodward, "Radar ambiguity analysis," Royal Radar Establishment, Malvern, U.K., Tech. Rep. RRE Tech. Note 731, 1967.

[18] A. W. Rihaczek, *Principles of High-Resolution Radar*. New York: McGraw-Hill, 1969.
[19] M. I. Skolnik, *Introduction to Radar Systems*, 2nd ed. New York: McGraw-Hill, 1980.
[20] N. Levanon, *Radar Principles*. New York: Wiley-Interscience, 1988.
[21] R. E. Blahut, W. Miller, Jr, and C. H. Wilcox, *Radar and Sonar: Part I*. New York: Springer-Verlag, 1991.
[22] J.-C. Guey and M. R. Bell, "Diversity waveform sets for delay-Doppler imaging," *IEEE Trans. Inf. Theory*, vol. 44, no. 4, pp. 1504–1522, Jul. 1998.
[23] R. A. Altes, "Some invariance properties of the wideband ambiguity function," *J. Acoustic. Soc. Amer.*, vol. 53, no. 4, pp. 1154–1160, Apr. 1973.
[24] L. H. Sibul and E. L. Titlebaum, "Volume properties for the wideband ambiguity function," *IEEE Trans. Aerosp. Electron. Syst.*, vol. AES-17, no. 1, pp. 83–87, Jan. 1981.
[25] Z. b. Lin, "Wideband ambiguity function of broadband signals," *J. Acoustic. Soc. Amer.*, vol. 83, no. 6, pp. 2108–2116, Jun. 1988.
[26] D. C. Lush and D. A. Hudson, "Ambiguity function analysis of wideband radars," in *Proc. 1991 IEEE Nat. Radar Conf.*, Los Angeles, CA, Mar. 12–13, 1991, pp. 16–20.
[27] P. Z. Peebles, Jr, *Radar Principles*. New York: Wiley-Interscience, 1998.
[28] G. S. Antonio, D. R. Fuhrmann, and F. C. Robey, "MIMO radar ambiguity functions," *IEEE J. Sel. Topics Signal Process.*, vol. 1, no. 1, pp. 167–177, Jun. 2007.
[29] A. I. Sinsky and C. P. Wang, "Standardization of the definition of the radar ambiguity function," *IEEE Trans. Aerosp. Electron. Syst.*, vol. AES-10, no. 4, pp. 532–533, Jul. 1974.
[30] C. H. Wilcox, "The synthesis problem for radar ambiguity functions," Univ. of Wisconsin, Madison, WI, MRC Tech. Summary Rep. 156, 1960.
[31] S. Sussman, "Least-square synthesis of radar ambiguity functions," *IRE Trans. Inf. Theory*, vol. 8, no. 3, pp. 246–254, Apr. 1962.
[32] D. DeLong and E. Hofstetter, "On the design of optimum radar waveforms for clutter rejection," *IEEE Trans. Inf. Theory*, vol. 13, no. 3, pp. 454–463, Jul. 1967.
[33] C. Stutt and L. Spafford, "A "best" mismatched filter response for radar clutter discrimination," *IEEE Trans. Inf. Theory*, vol. 14, no. 2, pp. 280–287, Mar. 1968.
[34] R. de Buda, "Signals that can be calculated from their ambiguity function," *IEEE Trans. Inf. Theory*, vol. 16, no. 2, pp. 195–202, Mar. 1970.
[35] O. Arikan and D. Munson, "Time-frequency waveform synthesis using a least-squares approach," in *Proc. IEEE Int. Symp. Circuits Syst.*, New Orleans, LA, May 1–3, 1990, vol. 1, pp. 242–245.
[36] I. Gladkova and D. Chebanov, "On a new extension of Wilcox's method," in *Proc. 5th WSEAS Int. Conf. Appl. Math.*, Miami, FL, 2004, pp. 1–6.
[37] I. Gladkova and D. Chebanov, "On the synthesis problem for a waveform having a nearly ideal ambiguity surface," presented at the 2004 Int. Radar Conf., Toulouse, France, Oct. 18–22, 2004.

Track-Before-Detect Strategies for STAP Radars

Danilo Orlando, Luca Venturino, Marco Lops, and Giuseppe Ricci

***Abstract*—In this correspondence we propose track-before-detect (TBD) strategies for space-time adaptive processing (STAP) radars. As a preliminary step we introduce the target and noise models in discrete-time form. Then, resorting to generalized likelihood ratio test (GLRT)-based and ad hoc procedures we derive detectors for two different scenarios (a point better clarified in the body of the correspondence). The preliminary performance assessment, conducted resorting to Monte Carlo simulation, shows that the proposed procedures might be viable means to implement early detection and track initiation of weak moving targets.**

***Index Terms*—Constant false alarm rate (CFAR), generalized likelihood ratio test (GLRT), space-time adaptive radar detection, track-before-detect (TBD), Viterbi algorithm.**

I. Introduction

Traditional tracking algorithms are designed assuming that the sensor provides a set of point measurements at each scan. In a radar system such measurements are obtained by thresholding the output of a matched filter fed by a baseband version of collected data [1]. An alternative approach, referred to as track-before-detect (TBD), consists of feeding the processor with unthresholded data. TBD-based procedures jointly process several consecutive scans (or frames) and, relying on a target kinematics or, simply, exploiting the physically admissible target transitions, jointly declare the presence of a target and, eventually, its track. A TBD algorithm can improve track accuracy and follow low signal-to-noise ratio (SNR) targets at the price of an increase of the computational complexity. Moreover, a TBD scheme ensuring the constant false alarm rate (CFAR) property with respect to the unknown statistics of the disturbance controls the overall false track acceptance probability (CFAR property at the track level).

Most of TBD algorithms have been proposed to detect and track small moving objects in optical images corrupted by high cluttered noise. Their use in connection with radar systems has received less attention: for a description of the existing results, see [2]–[5]. A family of low-complexity power-efficient TBD procedures has been presented in [4]. Therein, the continuous-time continuous-amplitude signal collected by a pulse Doppler radar is discretized to reflect the sectorization of the coverage area and the range gating operation, and the generalized likelihood ratio test (GLRT) is solved resorting to a Viterbi-like tracking algorithm. The proposed algorithm has a complexity linear in the number of integrated scans and in the time on target. The emphasis is on detection performance more than tracking: in fact, the GLRT does not rely on the target kinematics; it simply takes into account a maximum target velocity in order to define the admissible target transitions in range and azimuth (the Doppler is dealt with as a nuisance quantity due to the considered system and target parameters). However, a rough estimate of the target parameters is obtained as a by-product of the construction of the target statistic.

Manuscript received November 10, 2008; accepted August 21, 2009. First published September 25, 2009; current version published January 13, 2010. The associate editor coordinating the review of this manuscript and approving it for publication was Prof. Jean-Yves Tourneret.

D. Orlando, L. Venturino, and M. Lops are with the DAEIMI, Università degli Studi di Cassino, I-03043 Cassino (Fr), Italy (e-mail: danilo.orlando@unisalento.it; l.venturino@unicas.it; lops@unicas.it).

G. Ricci is with the Dipartimento di Ingegneria dell'Innovazione, Università del Salento, 73100 Lecce (Le), Italy (e-mail: giuseppe.ricci@unisalento.it).

Digital Object Identifier 10.1109/TSP.2009.2032991